Central European Geology, Vol. 60/2, 201–229 (2017)
DOI: 10.1556/24.60.2017.008
First published online September 12, 2017

The Budaörs-1 well revisited: Contributions to the Triassic stratigraphy, sedimentology, and magmatism of the southwestern part of the Buda Hills

János Haas[1]*, Tamás Budai[2], István Dunkl[3], Éva Farics[1], Sándor Józsa[4], Szilvia Kövér[1], Annette E. Götz[5], Olga Piros[2], Péter Szeitz[6]

[1]MTA-ELTE Geological, Geophysical and Space Science Research Group, Budapest, Hungary
[2]Geological and Geophysical Institute of Hungary, Budapest, Hungary
[3]Sedimentology and Environmental Geology, Geoscience Center, University of Göttingen, Göttingen, Germany
[4]Department of Petrology and Geochemistry, Eötvös Loránd University, Budapest, Hungary
[5]School of Earth and Environmental Sciences, University of Portsmouth, Portsmouth, United Kingdom
[6]Department of Paleontology, Eötvös Loránd University, Budapest, Hungary

Received: December 20, 2016; accepted: July 11, 2017

The 1,200-m-deep Budaörs-1 borehole provided important data for our understanding of the stratigraphy and tectonic setting of the southern part of the Buda Hills. Although previous reports contained valid observations and interpretations, a number of open questions remained. The importance of this borehole and the unsolved problems motivated us to revisit the archived core. The new studies confirmed the existing stratigraphic assignment for the upper dolomite unit (Budaörs Dolomite Formation) as the dasycladalean alga flora proved its late Anisian to Ladinian age assignment. An andesite dike was intersected within the Budaörs Dolomite. U–Pb age determination performed on zircon crystals revealed a Carnian age (~233 Ma), and settled the long-lasting dispute on the age of this dike, proving the existence of a Carnian volcanic activity in this area after the deposition of the Budaörs Dolomite. Palynostratigraphic studies provided evidence for a late Carnian to early Norian age of the upper part of the lower unit (Mátyáshegy Formation). This result verified an earlier assumption and reinforced the significance of the tectonic contact between the upper unit (Budaörs Formation) and the lower unit (Mátyáshegy Formation). Based on structural observations and construction of cross sections, two alternative models are presented for the structural style and kinematics of the contact zone between the Budaörs and Mátyáshegy Formations. Model A suggests a Cretaceous age for the juxtaposition, along an E–W striking sinistral transpressional fault. In contrast, model B postulates dextral transpression and an Eocene age for the deformation. The latter one is better supported by the scattered dip data; however, both scenarios are considered in this paper as possible models.

Keywords: Triassic stratigraphy, microfacies, andesite dike, tectonics, Buda Hills, Hungary

*Corresponding author: János Haas; MTA-ELTE Geological, Geophysical and Space Science Research Group, Eötvös Loránd University, Pázmány Péter sétány 1/c, H-1117 Budapest, Hungary
E-mail: haas@caesar.elte.hu

ISSN 1788-2281

Introduction

The Buda Hills are made up mostly of Triassic carbonate rocks, which are covered in places by relatively thin Cenozoic formations. In this area located in the outskirts of Budapest, the near-surface geology is well known due to geological investigations of more than 150 years. However, the database on the geology of the deeper subsurface is still poor, due to the limited number of deep core drillings. The Budaörs-1 (Bö-1) borehole, drilled in 1963 to explore the regional stratigraphic and structural setting, represents the deepest and most important well with core samples. The planners of the drilling project assumed that after intersecting the carbonates, the Werfen-type Lower Triassic would be penetrated; moreover, information on the presence and characteristics of the Permian succession and/or the crystalline basement were expected (Horváth and Némedi-Varga 1965). Although this pre-drill prognosis was not achieved by the well, the 1,200-m-deep drilling provided very significant data for understanding of the stratigraphy and structure of the southern part of the Buda Hills. Already the first report (Horváth and Némedi-Varga 1965) and a subsequent paper on the results of the performed investigations (Nagy et al. 1967) contained important observations and interpretations, which are still valid. However, a number of open questions remained since some of the problems could not be solved by the analytical methods available 50 years ago. The importance of this well and the unsolved problems motivated us to revisit the archived core and make a new analysis and an updated interpretation.

Geological setting

During the early stage of the Alpine plate tectonic cycle, the Transdanubian Range Unit was situated between the South Alpine and Austroalpine domains and arrived to its present-day position only by the early Miocene as the result of large-scale displacements (Schmidt et al. 1991; Csontos and Nagymarosy 1998; Csontos and Vörös 2004). In the Middle to Late Triassic, the area of the Buda Hills was located near the Neotethys shelf margin (Haas et al. 1995) where extensional basins begun to form in the Carnian.

Based on the characteristics of the Upper Triassic carbonates, three facies zones are distinguished within the area of the Buda Hills (e.g., Wein 1977; Haas et al. 2000). In the southern zone (Sas Hill facies belt), the Upper Triassic cherty dolomites of basin facies (Sashegy Dolomite Member of the Mátyáshegy Formation) occur that is probably underlain by the Middle Triassic platform carbonates of the Budaörs Dolomite (Figs 1 and 2). The northeastern zone (Hármashatár Hill facies belt) is also made up of a basinal succession (cherty dolomite, marl, and limestone of the Mátyáshegy Formation); its underlying formation is unknown. The central part of the Buda Hills (Jánoshegy facies belt) is characterized by Upper Triassic platform carbonates of the Fődolomit Formation and the oncoidal facies of the Dachstein Limestone (Fig. 2).

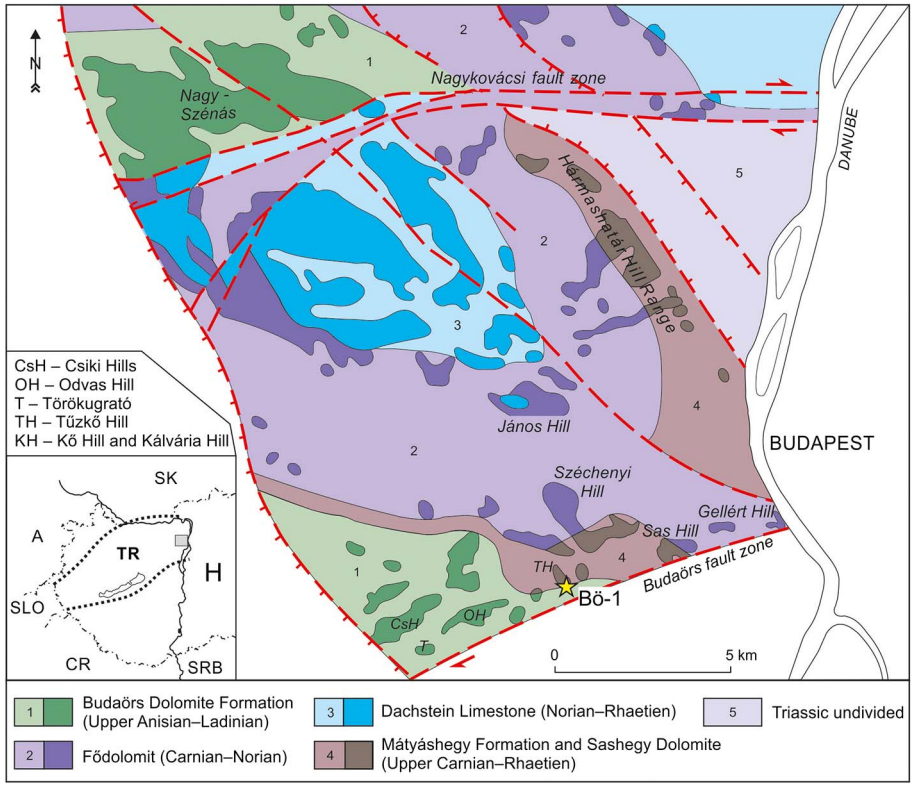

Fig. 1
Simplified pre-Cenozoic geological map of the Buda Hills (after Haas et al. 2000). (1) Budaörs Dolomite Formation (Upper Anisian–Ladinian); (2) Födolomit Formation (Carnian–Norian); (3) Dachstein Limestone Formation (Norian–Rhaetian); (4) Mátyáshegy Formation and Sashegy Dolomite Formation (Upper Carnian–Rhaetian); and (5) Triassic undivided. Bö-1 – Budaörs-1 well, CsH – Csiki Hills, KH – Kő Hill and Kálvária Hill, OH – Odvas Hill, T – Törökugrató Hill, TH – Tűzkő Hill

The Bö-1 well was drilled in a small abandoned quarry at the southern foot of the Tűzkő Hill (Fig. 3). The Tűzkő Hill belongs to the southern range of the Buda Hills, striking from the Csiki Hills in the west to the Gellért Hill in the east. This mountain range is made up mostly of Middle to Upper Triassic dolostones, which are directly overlain by Upper Eocene or Lower Oligocene deposits (Hofmann 1871; Schafarzik and Vendl 1929; Schréter et al. 1958; Wein 1977).

The oldest exposed formation of the Triassic succession is the Upper Anisian–Ladinian Budaörs Dolomite forming the main part of the Budaörs Hills. It contains a characteristic dasycladalean flora (*Diplopora annulata*) in several horizons (Hofmann 1871; Kutassy 1927). A peculiar bivalve fauna was found by Horusitzky (1959) from a quarry at the southern foot of the Tűzkő Hill, probably from the upper part of the

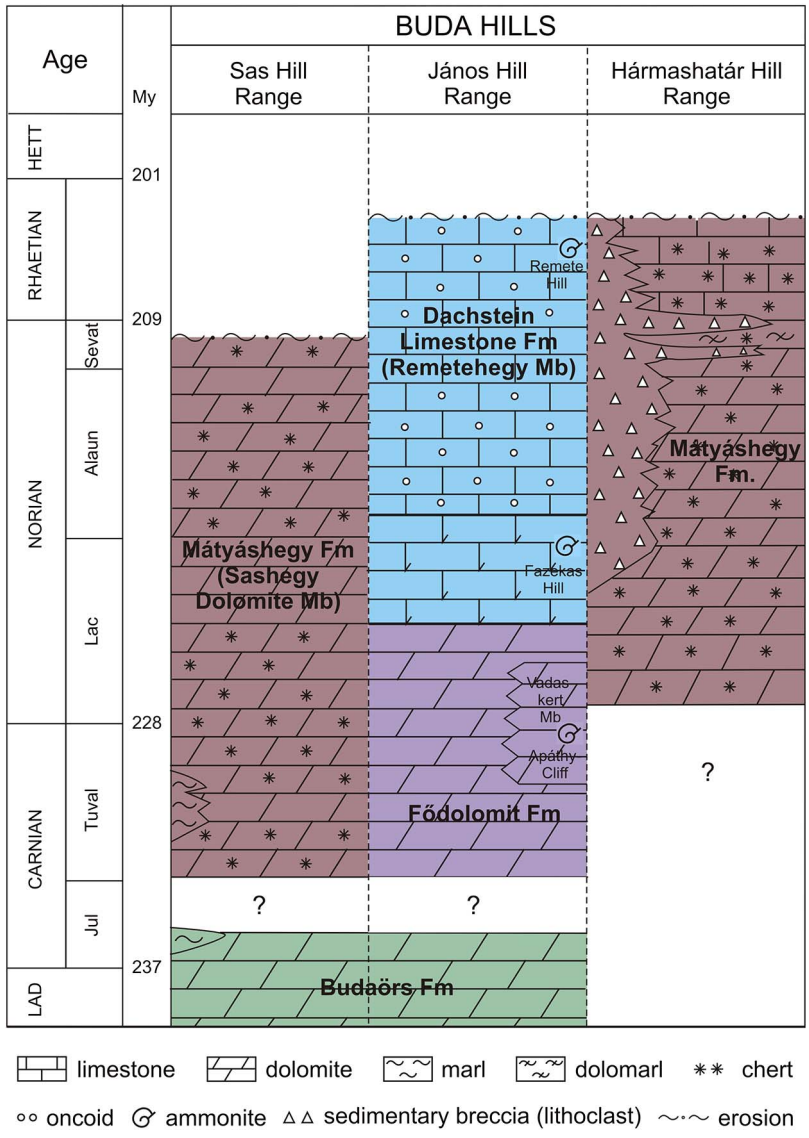

Fig. 2
Triassic stratigraphy of the Buda Hills showing the three Upper Triassic facies zones (*sensu* Wein 1977 and Haas et al. 2000)

formation; along with small megalodontids, *Avicula*, *Gervilleia*, and *Cassinella*. *Neomegalodon carinthiacus* and *Cuspidaria gladius* were reported by Végh-Neubrandt (1982) from the Tűzkő Hill, most probably from the same quarry.

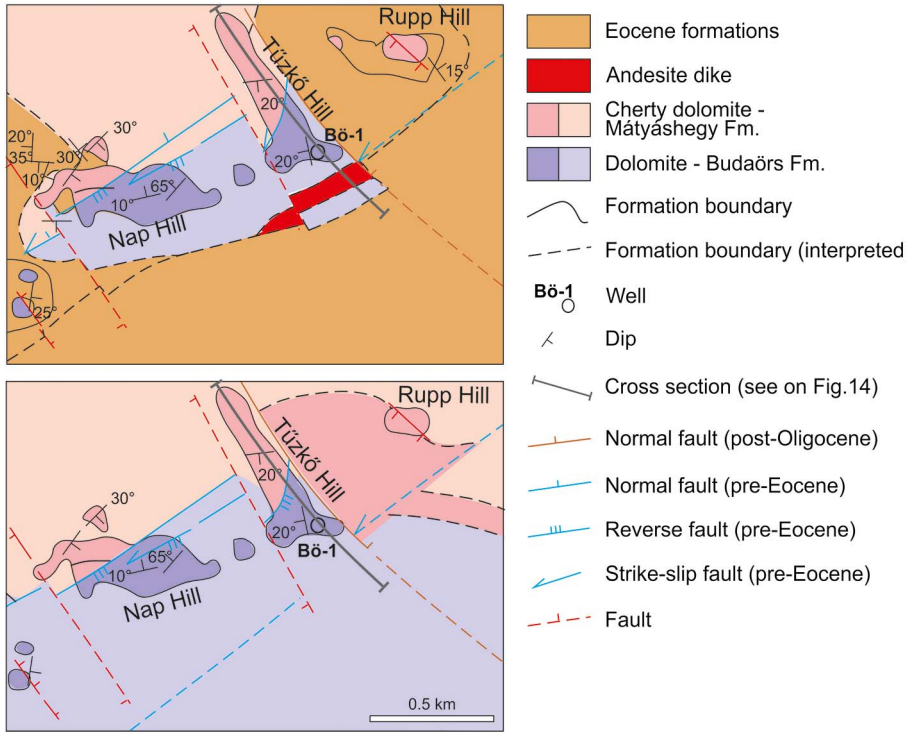

Fig. 3
Geological setting of the Budaörs-1 (Bö-1) well. (A) Pre-Cenozoic map. (B) Pre-Oligocene map (after Wein 1977, modified)

Cherty dolomite crops out in the northern part of the Tűzkő Hill, dipping southward with angles between 25° and 30°. This basinal facies belongs to the Sashegy Dolomite Member of the Mátyáshegy Formation (Fig. 3). Similar rocks can be followed in a narrow zone all along the southern range of the Buda Hills (Fig. 1). The samples collected from the northern part of the Tűzkő Hill yielded late Carnian–early Norian conodonts (Karádi et al. 2016). According to Vendl (1923), Végh-Neubrandt (1974), and Wein (1977), there is a tectonic contact between the Middle Triassic platform dolomite and the Upper Triassic cherty dolomite at the Tűzkő Hill.

In the Budaörs Hills, the Triassic formations are in places overlain by a deepening upward Upper Eocene sequence. The basal layers are made up of breccia and conglomerate containing rounded to subangluar clasts of dolomite and chert. In some places (Kálvária Hill and Kő Hill), a large amount of andesite clasts occurs in the basal beds (Hofmann 1871; Horváth and Tari 1987). Recent investigations pointed out that the petrographic features of these clasts are similar to those of the andesite dike found in core Bö-1 (Farics et al. 2015).

In places, the Upper Eocene conglomerate is overlain by a shallow marine Discocyclina-bearing limestone (Szépvölgy Formation), e.g., on the Törökugrató Hill. However, Triassic rocks are predominantly covered by the uppermost Eocene Buda Marl (Vendl 1923; Schafarzik and Vendl 1929; Magyari 1994, 1996). Lower Oligocene clays (Kiscell and Tard Formations) are preserved only locally. The Upper Miocene is represented by a fining-upward siliciclastic sequence (gravel, sand, silt, and clay) capped by freshwater limestone in some places (Schréter 1912; Schréter et al. 1958).

Materials and methods

Core drilling was applied for the major part of the borehole. Only two intervals between 0.0–60.0 and 92.0–120.0 m were penetrated by non-core drilling. In the dolomites, the core recovery was usually less than 40%, but in the andesite, it reached 85% to 100% (Horváth and Némedi-Varga 1965). From the preserved cores, 35 samples were taken for petrographic studies and paleontological investigations. About 170 thin sections from the archive of the Geological and Geophysical Institute of Hungary were also used for microfacies and micropaleontological studies of the carbonate rocks. For the petrographic investigation of the andesite, Olympus BH2 polarization microscope and AMRAY 1830 scanning electron microscope with EDAX PV 9800 ED spectrometer of the Eötvös Loránd University were used. For the classification of the magmatic rocks, Streckeisen's (1978) system was applied.

For the radiometric age determination, the zircon crystals were fixed on a double-side adhesive tape and embedded in a 25-mm diameter epoxy mount. The crystal mounts were lapped by 2,500 mesh SiC paper and polished by 9-, 3-, and 1-micron diamond suspensions. For all zircon samples and standards used in this study, cathodoluminescence (CL) images were obtained using a JEOL JXA-8900 electron microprobe at the Geoscience Center Göttingen to study their internal structure and to select homogeneous parts for *in situ* age determinations. The *in situ* U–Pb dating was performed by laser ablation single collector sector field inductively coupled plasma mass spectrometry (LA-SF-ICP-MS) at the Göchron Laboratory of the University of Göttingen. The method employed for analysis is described in detail by Frei and Gerdes (2009). A Thermo Finnigan Element 2 mass spectrometer coupled to a Resonetics excimer laser ablation system was used. All age data were obtained by single spot analyses with a laser beam diameter of 33 μm and a crater depth of approximately 10 μm. The laser was fired at a repetition rate of 5 Hz and at nominal laser energy output of 25%. Two laser pulses were used for pre-ablation. The carrier gases were He and Ar. Analytes of ^{238}U, ^{235}U, ^{232}Th, ^{208}Pb, ^{207}Pb, ^{206}Pb, mass204, and ^{202}Hg were measured by the ICP-MS. The age calculation and quality control are based on the drift and fractionation corrections by standard-sample bracketing using GJ-1 zircon reference material (Jackson et al. 2004). For further control, the Plešovice zircon (Sláma et al. 2008), the 91500 zircon (Wiedenbeck et al. 1995), and the

FC-1 zircon (Paces and Miller 1993) were analyzed as "secondary standards." The age results of the standards were consistently within 2σ of the published isotope dilution thermal ionization mass spectrometry (ID-TIMS) values. Drift and fractionation corrections and data reductions were performed by our in-house software (UranOS; Dunkl et al. 2008). The level of Hg-corrected ^{204}Pb signal was very low, thus no common lead correction was required. The concordia plots and age spectra were constructed by the help of Isoplot/Ex 3.0 (Ludwig 2012).

Palynological samples (Bö-1a, 1b, 1c, and 1d) from dark-gray, argillaceous dolomites span an interval of 52 m between 946- and 998-m depth. All samples were prepared using standard palynological processing techniques, including HCl (33%) and HF (73%) treatment for dissolution of carbonates and silicates, and saturated $ZnCl_2$ solution ($D \approx 2.2$ g/ml) for density separation. Residues were sieved at 15-μm mesh size. Slides have been mounted in Eukitt, a commercial, resin-based mounting medium and the sedimentary organic matter was studied under a Leica DM2000 transmitted light microscope.

Results

Stratigraphic assignment, lithology, and facies interpretation

Based on macroscopic features and microscopic texture of the studied section, two dolostone units are distinguished (Fig. 4). Light-gray finely to medium crystalline dolostone locally with stromatolite interbeds was found in the upper part (0–941 m) of the well. This unit was assigned to the Budaörs Dolomite Formation. Andesite was intersected within this formation between 775 and 831 m. The lower part of the well (below 941 m) is also made up of dolostone, but it strikingly differs to that of the upper part. Darker or lighter greenish gray finely crystalline locally laminated, argillaceous, in some intervals cherty dolostone was encountered in the lower part of the section. The upper part of this interval (941–1,080 m) shows characteristic features of the Mátyáshegy Formation. The assignment of the lowermost part of the well (below 1,080 m), which is made up of dark-gray finely crystalline dolomite is less unambiguous.

As already observed by Nagy et al. (1967), there is a tectonic contact between the Budaörs and the Mátyáshegy Formations at 941 m, and a strongly fractured and brecciated interval occurs directly above it (910–941 m). The andesite interval is also bounded by tectonic contacts.

Budaörs Dolomite

On the basis of its lithological features, the exposed part of the Budaörs Formation can be subdivided into two units (Fig. 4). In the upper unit (0–420 m), fabric-preserving dolomite of microbial boundstone fabric alternates with biomicrite wackestone or

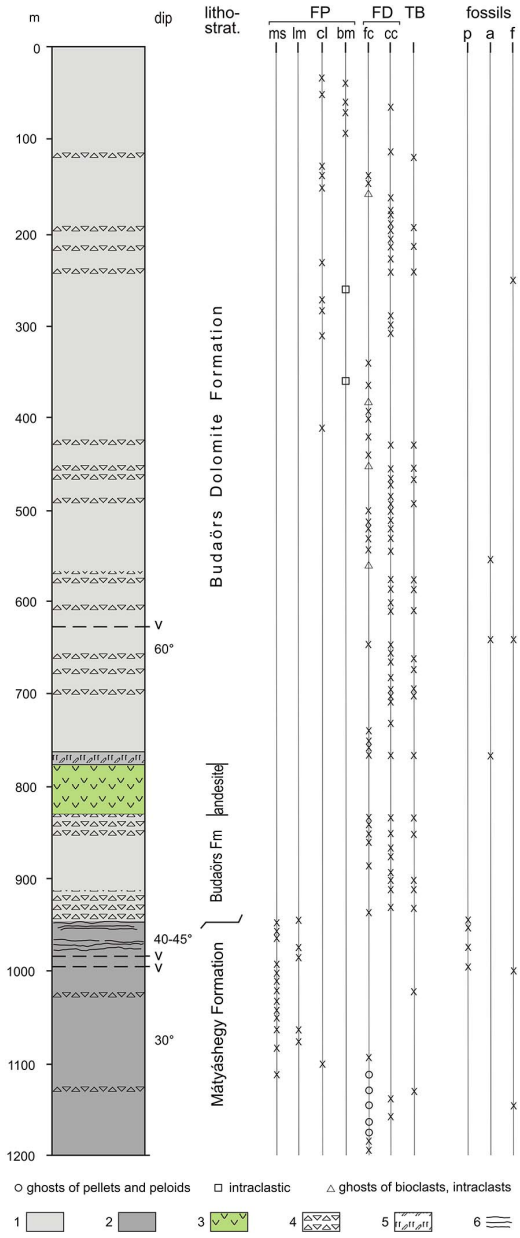

Fig. 4
Stratigraphic column of the Budaörs-1 core. Microfacies: FP – preserved sedimentary fabric, FD – destructed sedimentary fabric, TB – tectonic breccia, ms – mudstone, lm – laminated mudstone, cl – clotted microbial fabric, bm – bioclastic mudstone, fc – finely crystalline, cc – coarsely crystalline, Fossils: p – palynomorphs, a – algae, f – Foraminifera. Legend: (1) dolomite of platform facies; (2) dolomite of basin facies; (3) andesite; (4) tectonic breccia; (5) contact zone; and (6) lamination

fabric-destructive finely crystalline dolomite. The microbial boundstone lithofacies has a fenestral laminated microstructure with clotted microsparitic fabric. Finely to medium crystalline dolomite cement occludes the fenestral pores (Fig. 5). Geopetal filling was encountered in some larger pores, where very finely crystalline dolomite mudstone is covered by medium crystalline dolomite cement (Fig. 6). In the biomicrite wackestone microfacies, the scattered molds of mollusc fragments and Foraminifera are filled by finely to medium crystalline dolomite cement. Coarsely crystalline dolomite also occurs generally in the strongly fractured and brecciated intervals. In the lower unit of the Budaörs Formation (420–941 m), exclusively fabric-destructive dolomite was found. The less fractured and brecciated intervals are characterized by finely crystalline dolomites, locally with ghosts of grains, although medium to coarsely crystalline rocks also occur. In the intensely fractured and brecciated intervals, the medium to coarsely crystalline dolomite is prevailing.

Specimens of dasycladalean algae were found in some samples from the middle part of the exposed section of the Budaörs Formation (Fig. 7). ?*Anisoporella* sp. and

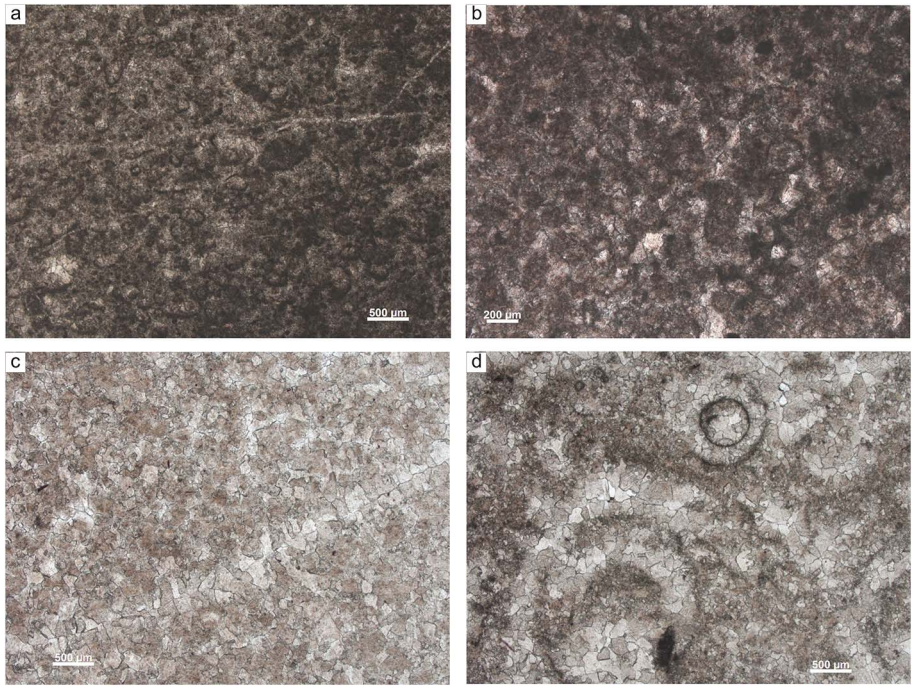

Fig. 5
Microfacies types of the Budaörs Dolomite. (a) Finely crystalline dolomite with ghosts of sand-sized grains (340 m). (b) Finely to medium crystalline dolomite with ghosts of sand-sized grains (bioclasts and peloids, 364 m). (c) Medium to coarsely crystalline, planar-s, fabric distructive dolomite (514 m). (d) Medium to coarsely crystalline, planar-s, fabric-destructive dolomite with ghosts of dasycladalean algae (546 m)

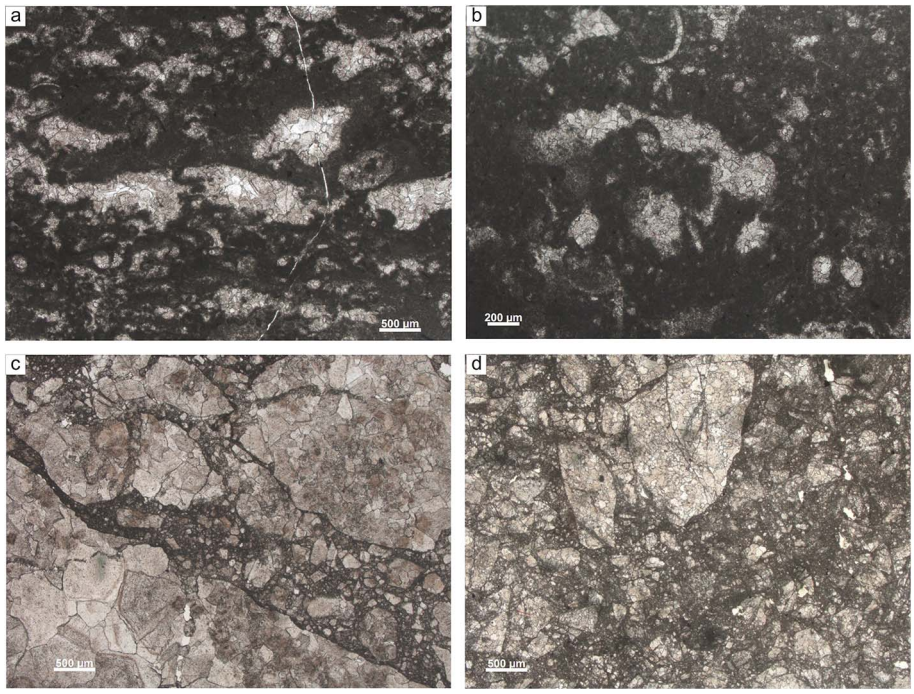

Fig. 6
Microfacies types of the Budaörs Dolomite. (a and b) Fabric-preserving dolomite: microbial boundstone with fenestral pores. The pores are lined by very fine crystalline, the pore centers are filled by medium crystalline dolomite cement (272 and 228 m). (c) Dolomite breccias: mm- to cm-sized clasts of coarsely crystalline dolomite in pulverized microcrystalline dolomite matrix (465 m). (d) Dolomite breccias: 0.5 mm- to cm-sized clasts of medium crystalline dolomite in pulverized microcrystalline dolomite matrix (765 m)

?*Physoporella* sp. were encountered at 552 m. *Diplopora annulata* was determined from 639 m and *Acicularia* sp. from 765 m. Since the range of *D. annulata* is late Anisian to Ladinian (Piros and Preto 2008), these data seem to confirm the Ladinian age assignment of Nagy et al. (1967) for the upper part of the core. A few Foraminifera were also encountered (Fig. 7). *Aulotortus cf. sinuosus* was found at 251 m along with *Textularia?* sp. and *Endothyra keuperi* at 645 m. *Aulotortus sinuosus* occurs already in the Anisian (Brönniman et al. 1973; Piller 1978) and it is a characteristic species of platform associations until the end of the Triassic (Chablais et al. 2011; Gale 2012). It is included in Oravecz-Scheffer's (1987) list of the common Triassic Foraminifera species of the Transdanubian Range with a range from the late Ladinian to Rhaetian. *Endothyra keuperi* was described from the Carnian (Oberhauser 1960) and its stratigraphic range certainly encompasses the Anisian to Carnian interval (Koehn-Zaninetti 1969; Kolar-Jurkovšek et al. 2005; Pelech et al. 2012). According to Oravecz-Scheffer (1987), this species also occurs in the Transdanubian Range from the late Anisian to the end of the Triassic. Accordingly, the stratigraphic ranges of these

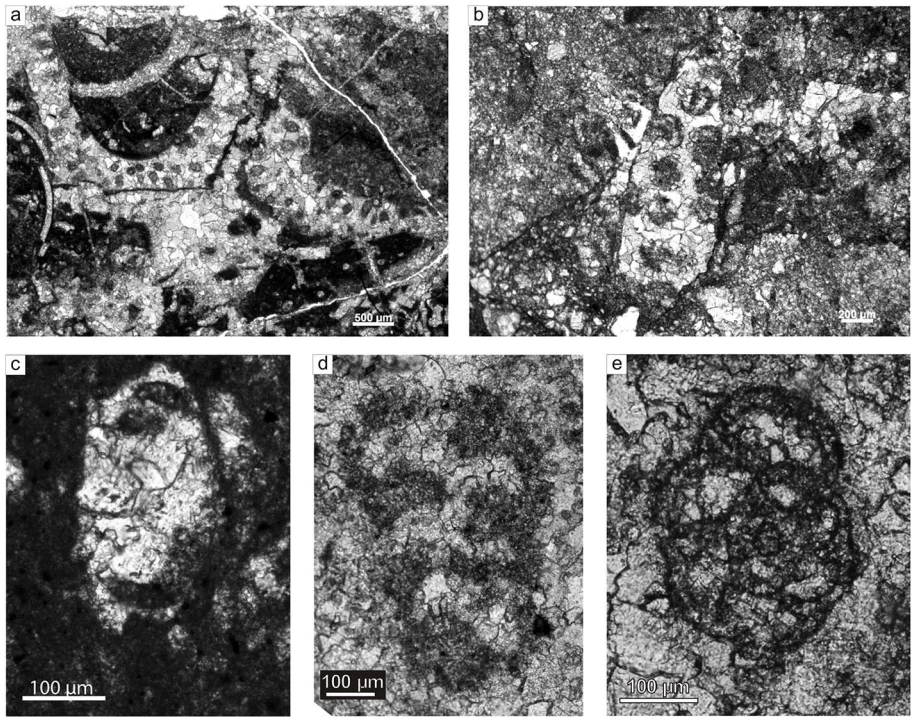

Fig. 7
Dasycladaleans and Foraminifera of the Budaörs Dolomite. (a) *Diplopora annulata* (639 m). (b) *Acicularia* sp. (765 m). (c) *Aulotortus cf. sinuosus* (251 m). (d) *Textularia?* sp. (645 m). (e) *Endothyra keuperi* (645 m)

species are not in conflict with the late Anisian to Ladinian (earliest Carnian?) age assignment of this formation.

The Budaörs Formation intersected in core Bö-1 shows similar characteristics as described from its surface exposures at Odvas Hill, Budaörs (Hips et al. 2015), close to the drilling site. Consequently, inferences of these studies can be applied for interpretation of the depositional conditions and diagenetic processes. According to Hips et al. (2015), sea-level oscillation led to deposition of shallowing-upward cycles on a large carbonate platform. Bioclastic carbonates were deposited during the higher sea-level periods in shallow subtidal environments. Sea-level fall led to progradation of tidal flat environment widely covered by microbial mats where synsedimentary organogenic dolomite formation may have taken place. It was followed by near-surface replacive dolomitization producing finely crystalline dolomite. Replacive dolomitization in intermediate burial setting produced medium crystalline dolomite and resulted in complete dolomitization of the formation (Hips et al. 2015). Tectonic processes led to formation of fault zones that facilitated the fluid transport, precipitation of coarsely crystalline dolomite in the fractures, and recrystallization of the previously

formed dolomite phases to coarser crystal size in the vicinity of fault zones. These dolomite-forming processes must have taken place prior to the late Eocene, since all of the above-described rock types appear in the Eocene basal conglomerate.

Andesite dike

An andesite interval was intersected within the Budaörs Dolomite between a depth of 773 and 831.4 m. Although this is bound by tectonic contacts, the position of the magmatic rocks suggests that it is a dike. This interpretation is supported by the observation of Horváth and Némedi-Varga (1965) who reported strongly altered dark-gray silicified and pyritized rocks just above the upper contact of the andesite interval.

The black and green andesite is made up of dense, fine-grained groundmass in which sprinkled phenocrysts of feldspar and mafic minerals (or their pseudomorphs) occur. There is a shear zone between ca. 779 and 781 m within the andesite that consists of slightly oriented angular, only weakly altered andesite rock fragments (2–5 mm) in a fine-grained matrix. Above the shear zone, the andesite is fresh or only weakly altered, whereas below this zone, it is strongly altered as a result of K-metasomatism showing downward increasing intensity.

The andesite has porphyric pilotaxitic and less frequently trachytic texture. The amount of glass is maximum 10%. It consists of 25%–30% of phenocrysts, ca. 70% of them plagioclase, ca. 30% hypersthene, and less than 1% augite (Fig. 8). The most common accessories are ilmenite (leucoxene), apatite, garnet, magnetite, zircon, and monazite. Determined by electron microprobes, the composition of 1–3 mm plagioclases is labradorite/andesine. They commonly show zoning. The plagioclases commonly contain mafic minerals, pseudomorphs after mafic minerals, apatite, rutile, and opaque minerals as inclusions. The upper part of the volcanic rock interval (ca. 773–781 m) contains fresh or weakly sericitized plagioclase. The lower part of this interval (ca. 781–831 m) is composed of weakly or strongly altered plagioclases. The effect of K-metasomatism appears as rims of K-feldspar on plagioclase crystals. The core of some of the plagioclase phenocrysts is replaced by kaolinite. The hypersthene is 1–2 mm; the augite is 0.5–1 mm in size. They show mostly hipidiomorphic or rarely idiomorphic crystal faces. Hypersthene contains apatite and ilmenite inclusions. Unaltered pyroxene was found only in the uppermost part of the volcanic rock interval (above 773 m). Elsewhere the pseudomorphs after pyroxene are filled either by chlorite, clay, and opaque minerals (in the upper part) or by chlorite, nontronite, other clay minerals, opaque minerals, quartz, chalcedony, and carbonate (in the lower part). The pseudomorphs are commonly surrounded by opacite rims.

In the groundmass, lath-shaped microlites – predominantly plagioclase, subordinately biotite or chlorite after biotite – occur in a glass-poor mesostasis (maximum 10% of glass, Fig. 8b). The plagioclase is andesine/oligoclase, which is more acidic than the phenocrysts. Sericite is a common alteration phase in the plagioclase laths. The laths are occasionally oriented mostly along the phenocrysts. The glass is altered to chlorite, clay minerals (mostly glauconite), and rarely to carbonate. Ilmenite and

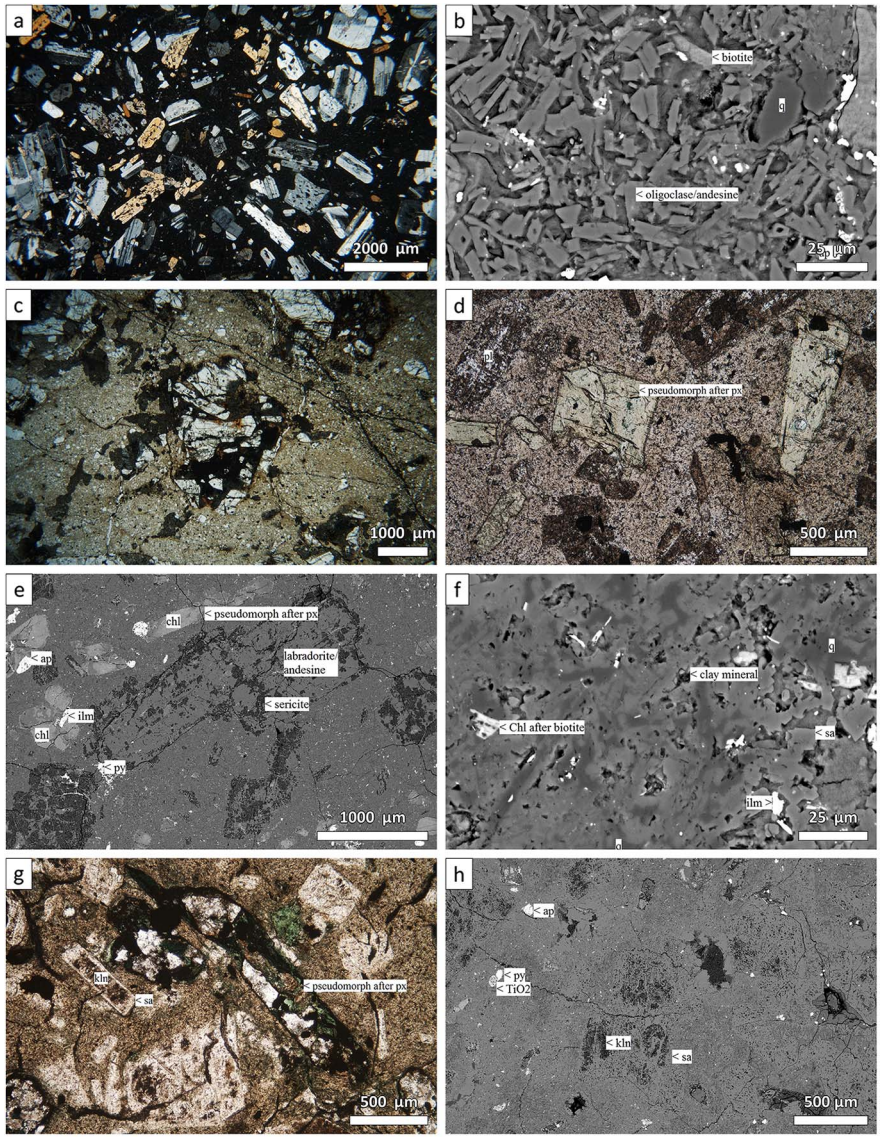

Fig. 8
Petrographic features of andesite in the Budaörs-1 core. (a) Texture of fresh andesite (2N, 773 m). (b) Texture of fresh groundmass [backscattered electrons (BSE) image, 775.9 m]. (c) Tectonic breccia in the shear zone (1N, 779.5 m). (d) Andesite with strongly sericited plagioclase and pseudomorphs after pyroxene (1N, 790.4 m). (e) Texture of andesite with sericited plagioclase and pseudomorph after pyroxene (BSE image, 790.4 m). (f) Strongly altered groundmass – secondary silica, effect of K-metasomatism (BSE image, 790.4 m). (g and h) Texture of andesite rims of K-feldspar along plagioclase (K-metasomatism) and pseudomorph after pyroxene (g: 1N, 808 m and h: BSE image, 807.6 m). px – pyroxene, q – quartz, sa – sanidine, kln – kaolinite, chl – chlorite, ap – apatite, py – pyrite, ilm – ilmenite

apatite also occur in the groundmass. In the lower part of the volcanic interval, the K-metasomatism replaced the plagioclase laths by K-feldspar. Continuous downward increase of secondary silica was observed in the groundmass. It has mosaic texture with opaque minerals and limonite–hematite.

The andesite contains some microdiorite inclusions, composed of the same minerals as the andesite. The fractures of the andesite are mostly filled by chalcedony, carbonate, and quartz with pyrite.

Two andesite samples (from 604 to 790.4 m) contain zircon crystals suitable for laser ablation LA-SF-ICP-MS U–Pb geochronology. The analytical details are in Table 1 and the characteristic CL pattern of the zircons is presented in Fig. 9. The concordant $^{206}Pb/^{238}U$ ages in the sample from 604 m show an extremely wide scatter from 235 to 543 Ma (Fig. 10a). This zircon concentrate was produced from a small-sized drilling core and thus no more zircon grains were available to identify more precisely the age components. The scatter derives from inherited, old cores of zircons, and their high proportion indicates that the andesitic melt consumed older continental crust.

The sample from 790.4 m yielded more consistent age information, however, it was not possible to extract a concordant age from the 18 single-spot ages (Fig. 10b). Here only one discordant Carboniferous crystal occurred, the rest of the data is Triassic. Some characteristic sample means age can be expressed by the lower intercept on the concordia plot (230.4 ± 4.0 Ma) and also by the Tukey's biweight mean (232.8 ± 3.6 Ma). The later was calculated by considering only the ages having less than 5% discordance (10 from the 17 Triassic ages).

The Carnian age of the andesite dike is only slightly younger than the Ladinian host rock. This igneous activity probably belongs to the Middle–Late Triassic magmatic suite that is mostly exposed in the Southern Alps (e.g., Sloman 1989).

Mátyáshegy Formation

The lower part of the core can also be subdivided into two units (Fig. 4). The upper unit (941–1,111 m) is characterized by aphanocrystalline to very finely crystalline, usually fabric-preserving dolomite. It is argillaceous mostly in the upper part of this segment and locally siliceous, cherty, mostly in its lower part. The argillaceous rock types are commonly laminated and punctuated by clayey horizons (Fig. 11). Alternation of silt size bioclastic and micrite mudstone laminae is also visible. Carbonate nodules occur in clayey matrix in some layers. Very few bioclasts (tiny echinoderm fragments, molds of bivalves, ostracods, and spine spicules) can be recognized in the mudstone (Fig. 11).

Palynostratigraphy reveals a Norian age for the sample taken from 946 m with palynomorph assemblage A including *Perinopollenites elatoides, Patinasporites densus, Corollina* sp., whereas the samples taken from 949, 970, and 998 m show a late Carnian age with palynomorph assemblage B including *Riccisporites tuberculatus, P. densus, Triadispora verrucata, Corollina* sp. Generally, the preservation of palynomorphs is poor to very poor, which might be related to structural movements and (?) hydrothermal fluids.

Table 1
Detailed results of the single-grain U–Pb geochronology obtained on the dikes of the studied Budaörs-1 borehole

Depth (m)	Grain ID	U (ppm)	Pb (ppm)	Th/U	^{206}Pb (%)	^{208}Pb/^{206}Pb	^{206}Pb/^{238}U	±1σ (%)	^{207}Pb/^{235}U	±1σ (%)	^{207}Pb/^{206}Pb	±1σ (%)	ρ	^{206}Pb/^{238}U	±2σ (Ma)	^{207}Pb/^{235}U	±2σ (Ma)	^{207}Pb/^{206}Pb	±2σ (Ma)	Disc. I. (%)	Disc. II. (%)
604	184	147	128	1.00	1.8	0.348	0.096386	0.9	0.9886	2.2	0.0744	2.0	0.42	593.2	10.3	698	22.1	1052	40.2	15	43.6
	185	177	76	0.50	0.0	0.163	0.0837062	0.8	0.6704	2.2	0.0581	2.0	0.38	518.2	8.4	521	18.1	533.2	45.1	0.5	2.8
	186	192	240	1.44	0.2	0.484	0.0878321	1.0	0.7306	2.2	0.0603	2.0	0.44	542.7	9.9	556.9	18.9	615.4	42.8	2.5	11.8
	187	311	112	0.42	0.0	0.134	0.0420723	0.9	0.3011	2.5	0.0519	2.3	0.37	265.7	4.7	267.3	11.7	281.6	53	0.6	5.7
	188	218	98	0.51	0.7	0.177	0.0379438	0.9	0.2957	2.6	0.0565	2.4	0.35	240.1	4.3	263.1	12	473.1	53.5	8.7	49.3
	189	175	55	0.37	1.2	0.149	0.0352217	1.0	0.2933	3.2	0.0604	3.0	0.3	223.1	4.2	261.2	14.7	617.8	65.6	14.6	63.9
	190	145	38	0.30	0.1	0.095	0.0733746	0.9	0.5776	2.7	0.0571	2.5	0.35	456.5	8.1	462.9	19.8	495.1	55	1.4	7.8
	191	73	136	2.14	0.2	0.677	0.0804545	1.1	0.6510	3.3	0.0587	3.1	0.33	498.8	10.4	509.1	26.4	555.4	67.7	2	10.2
	192	120	45	0.43	0.2	0.148	0.0371934	1.3	0.2704	3.3	0.0527	3.0	0.39	235.4	5.9	243	14.1	317.1	68.1	3.1	25.8
	193	1,836	1436	0.88	17.7	0.493	0.0349888	0.7	0.9254	1.7	0.1918	1.6	0.42	221.7	3.2	665.2	16.8	2758	26.5	66.7	92
	194	253	79	0.36	n.d.	0.122	0.052559	0.8	0.3759	2.2	0.0519	2.1	0.38	330.2	5.4	324	12.3	279.8	47.2	−1.9	−18
	195	1,114	156	0.16	1.7	0.042	0.052199	0.7	0.4782	1.9	0.0665	1.7	0.39	328	4.7	396.9	12.5	820.5	36.7	17.3	60
790.4	161	144	42	0.34	0.9	0.135	0.0365375	1.1	0.2931	3.2	0.0582	3.1	0.33	231.3	4.9	261	15	536.6	67	11.4	56.9
	162	87	28	0.37	0.5	0.127	0.034938	1.4	0.2626	5.1	0.0545	4.9	0.27	221.4	6.0	236.8	21.5	392.2	109	6.5	43.6
	163	150	62	0.47	0.2	0.158	0.0363616	1.3	0.2624	3.4	0.0523	3.1	0.4	230.2	6.0	236.6	14.2	300.5	70.3	2.7	23.4
	164	183	62	0.39	0.1	0.123	0.0366402	1.1	0.2618	2.9	0.0518	2.7	0.38	232	5.1	236.1	12.3	277.2	61.8	1.7	16.3
	165	344	160	0.54	0.0	0.173	0.0376895	0.8	0.2633	2.3	0.0507	2.1	0.37	238.5	4.0	237.4	9.8	226.1	49.6	−0.5	−5.5
	166	115	44	0.44	n.d.	0.133	0.0371085	1.1	0.2558	3.2	0.0500	3.0	0.35	234.9	5.3	231.3	13.4	194.7	70.1	−1.6	−20.6

(Continued)

Table 1 *(Continued)*

Depth (m)	Grain ID	U (ppm)	Pb (ppm)	Th/U	^{206}Pb (%)	^{208}Pb/^{206}Pb	^{206}Pb/^{238}U	±1σ (%)	^{207}Pb/^{235}U	±1σ (%)	^{207}Pb/^{206}Pb	±1σ (%)	ρ	^{206}Pb/^{238}U	±2σ (Ma)	^{207}Pb/^{235}U	±2σ (Ma)	^{207}Pb/^{206}Pb	±2σ (Ma)	Disc. I. (%)	Disc. II. (%)
	167	129	43	0.39	n.d.	0.139	0.0360168	1.0	0.2450	3.2	0.0493	3.0	0.32	228.1	4.5	222.5	12.7	163.7	70.2	−2.5	−39.3
	168	171	57	0.38	0.6	0.131	0.0353225	1.1	0.2693	3.2	0.0553	3.0	0.34	223.8	4.7	242.1	13.7	424.3	66.5	7.6	47.3
	169	185	74	0.46	n.d.	0.143	0.0377392	0.9	0.2603	2.8	0.0500	2.7	0.32	238.8	4.2	234.9	11.8	196.1	61.7	−1.7	−21.8
	170	61	21	0.39	3.4	0.207	0.0387921	1.3	0.4203	6.7	0.0786	6.6	0.19	245.3	6.2	356.2	40.7	1162	131	31.1	78.9
	171	227	64	0.33	0.1	0.103	0.0369027	1.0	0.2611	3.1	0.0513	3.0	0.31	233.6	4.4	235.5	13.2	254.8	68.5	0.8	8.3
	172	158	74	0.54	1.0	0.193	0.0346601	1.0	0.2782	3.0	0.0582	2.9	0.31	219.6	4.1	249.3	13.5	538.3	63.2	11.9	59.2
	173	140	41	0.34	6.0	0.229	0.0386918	1.0	0.5279	2.9	0.0990	2.8	0.33	244.7	4.7	430.4	20.8	1605	52.2	43.1	84.7
	174	117	20	0.21	2.1	0.091	0.0496241	10.8	0.4771	15.6	0.0697	11.3	0.69	312.2	66.0	396.1	105	920.3	231	21.2	66.1
	175	132	44	0.38	n.d.	0.127	0.0366825	1.0	0.2546	3.4	0.0503	3.2	0.31	232.2	4.7	230.3	13.9	210.7	74.1	−0.8	−10.2
	181	299	125	0.48	0.2	0.159	0.0372798	0.9	0.2685	2.7	0.0522	2.5	0.34	235.9	4.3	241.5	11.6	295.8	57.7	2.3	20.2
	182	139	48	0.40	1.4	0.143	0.0376322	1.1	0.3222	3.8	0.0621	3.6	0.29	238.1	5.1	283.6	18.8	677.8	77.4	16	64.9
	183	232	84	0.42	0.2	0.135	0.0349544	0.9	0.2509	2.5	0.0521	2.4	0.34	221.5	3.7	227.3	10.3	288.2	54.1	2.6	23.2

U and Pb content and Th/U ratio were calculated according to the nominal concentrations of GJ-1 reference zircon

Corrected isotope ratios: background extracted, drift and fractionation from the nominal ID-TIMS value of GJ-1 reference

The ^{207}Pb/^{235}U ratio is calculated by the corrected 7/6 and 6/8 ratios as ^{207}Pb/^{206}Pb/(^{238}U/^{206}Pb × 1/137.88)

The ρ is the ^{206}Pb/^{238}U/^{207}Pb/^{235}U error correlation coefficient

Discordance I is calculated as 100 × [1 − (^{206}Pb/^{238}U age)/(^{207}Pb/^{235}U age)] and Discordance II as 100 × [1 − (^{206}Pb/^{238}U age)/(^{207}Pb/^{206}Pb age)]

n.d.: not detectable

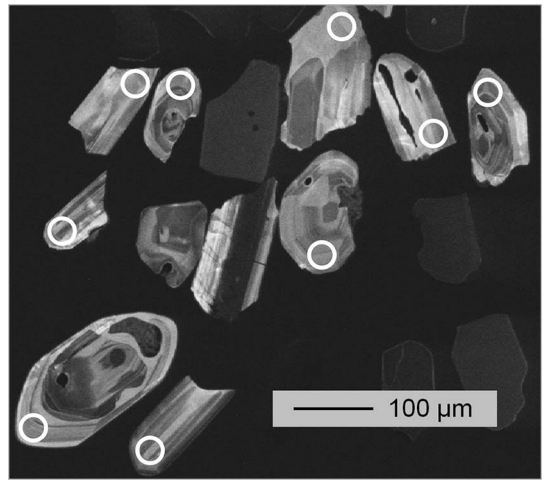

Fig. 9
Cathodoluminescence image of polished zircon crystals from the andesite dike of the studied Bö-1 borehole (790.4 m). Besides the well-developed, mostly euhedral shape, and the oscillatory zoning, the relatively voluminous, irregular patches with low CL intensity are also typical for the zircons. White circles represent the positions of laser ablation spots

Relatively well-preserved specimens of Foraminifer *Ammodiscus incertus* were found at 1,000 m (Fig. 12). *Ammodiscus* species are extremely persistent, they occur from the Paleozoic to the present. They typically thrive in low-energy shallow marine environment affected by fine siliciclastic input.

For conodont investigation, seven samples from the interval between 945.0 and 1,055 m were dissolved by acetic acid; not one yielded conodonts. However, in this context, it is worth mentioning that the samples collected in the outcrops of the Tűzkő Hill (Fig. 3) from cherty dolomites lithologically similar to those of the sampled interval, conodonts indicating the Carnian/Norian boundary interval were encountered (Karádi et al. 2016).

Finely crystalline dolomite with well-preserved fecal pellets (Fig. 9) occurs in the uppermost part of the lower unit (1,111–1,200 m). The sedimentary fabric is usually destructed in the deeper part of the core, but pellet or peloid grains are still identifiable. The abundance of fecal pellets and peloid grains suggests a relatively shallow marine depositional environment. A single specimen of Foraminifer *Hoyenella sinensis* was encountered at 1,145 m (Fig. 12). This cosmopolitan species was reported from many Lower to Middle Triassic formations (Rettori 1994, 1995; Rychliński et al. 2013). However, Oravecz-Scheffer (1987) found this species in the Middle to late Norian Feketehegy Formation in the NE part of the Transdanubian Range. Finely to medium crystalline fabric-destructive planar-s dolomite with irregular aphaneritic dolomite mottles occurs at the lowermost part of the core section.

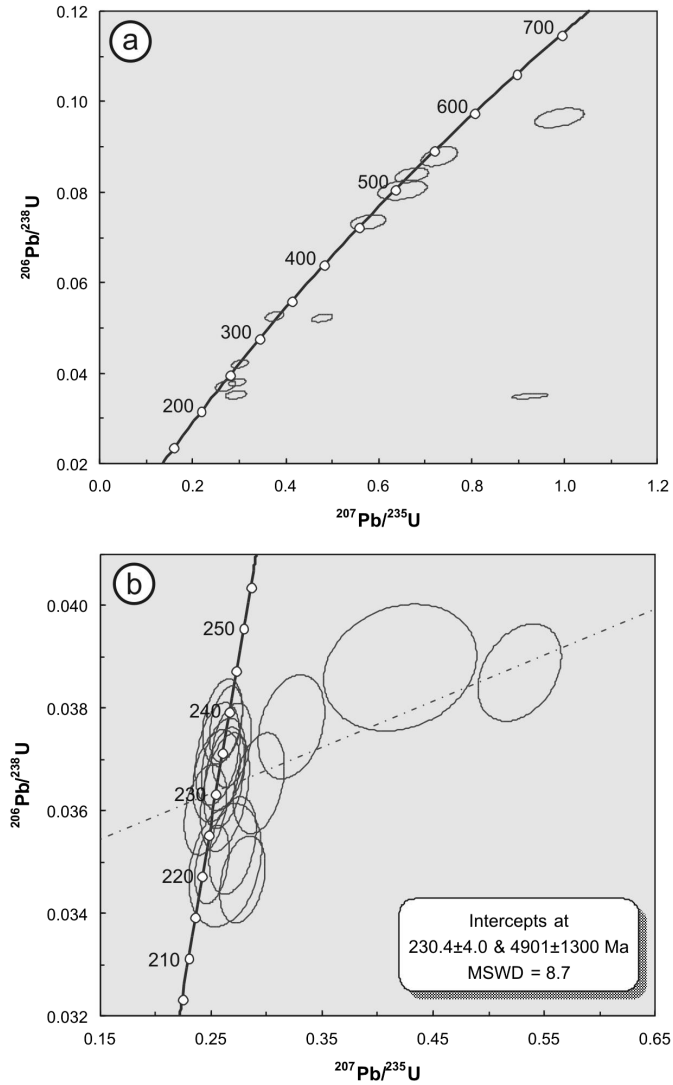

Fig. 10
Wetherill plot of LA-ICP-MS zircon U–Pb ages from the andesite dikes of the studied Budaörs-1 borehole. (a) In the sample from 604-m depth, the concordant, inherited grains are dominating. (b) In the sample from 790.4-m depth besides the Triassic grains, there was only one older zircon

Structural observations

Several tectonic breccia zones occur in the intersected section of the Budaörs Formation. They were documented already in the first report of Horváth and

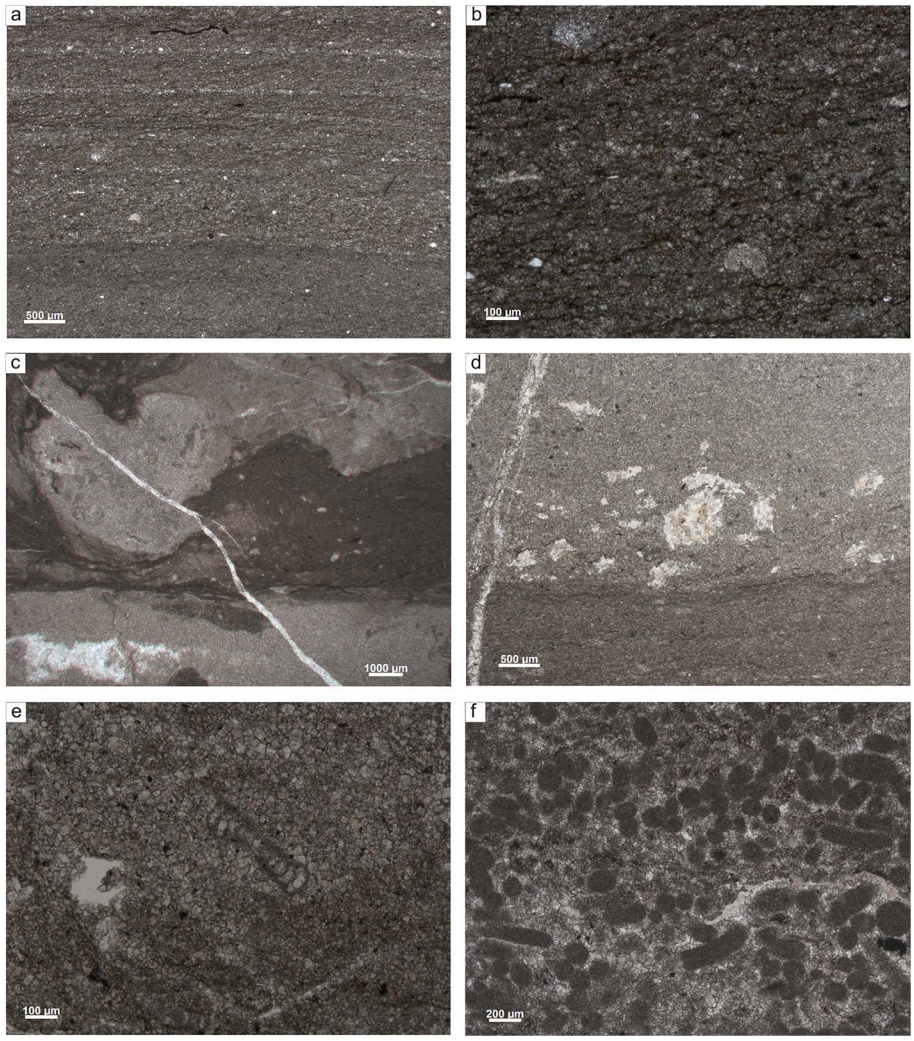

Fig. 11
Microfacies types of the Mátyáshegy Formation. (a) Laminated mudstone: it is made up of an alternation of micrite and bioclastic calcisilt laminae (943 m). (b) Calcisilt lamina: a small crinoid fragment (C) is recognizable (943 m). (c) Nodular argillaceous dolomite mudstone (948 m). (d) Dolomite mudstone with small silicified mottles (975 m). (e) Finely crystalline dolomite: the sedimentary texture is mostly destructed, but the Foraminifera tests are well-preserved (1,000 m). (f) Finely crystalline dolomite with fairly well-preserved fecal pellets (1,111 m)

Némedi-Varga (1965) and in the paper of Nagy et al. (1967). Tectonic breccia of various clast sizes was observed in the thin sections derived from these intervals (Fig. 4). In the present study, the lower part of the well (below 700 m) was the focus of the

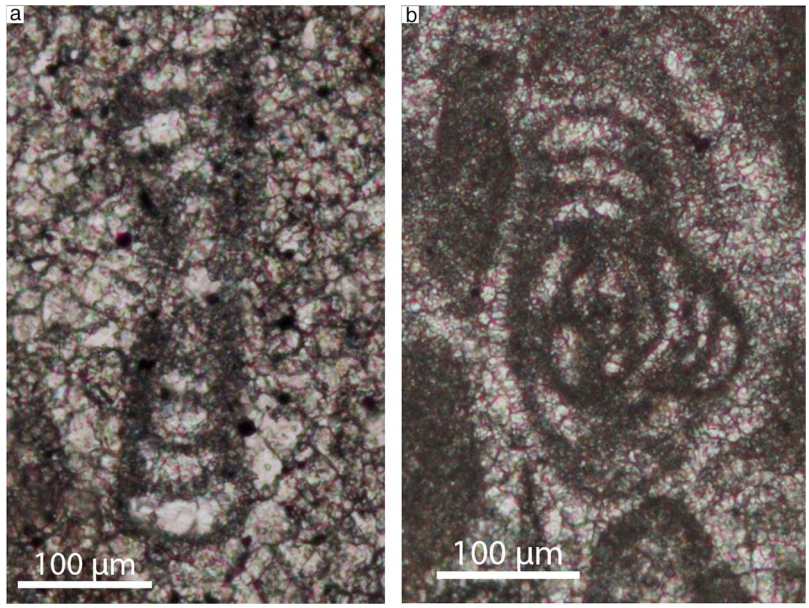

Fig. 12
Foraminifera in the Mátyáshegy Formation. (a) *Ammodiscus incertus* (1,000 m). (b) *Hoyenella sinensis* (1,145 m)

structural observations, due to the significance of the structural setting of the magmatic dike and contact of the Budaörs Dolomite and the Mátyáshegy Formation.

Between 765 and 767 m, a wide tectonic breccia zone was penetrated. The light-gray dolomite forms mm- to cm-scale angular breccia clasts, which is surrounded by sparry calcite and dolomite cement. Subvertical faults cut through the breccia with highly oblique slickenside lineation (Fig. 13a).

A few meter-wide breccia zone occurs at the upper contact of the andesite dike and the dolomite host rock. The dolomite is crushed into mm-scale fragments, which is surrounded by powdered dolomite. The breccia is loosely cemented. Within the andesite dike, some subvertical fault planes are detected with dip-slip slickenside lineation. Close to the lower contact of the andesite and the dolomite, a flat fault plane was detected with subhorizontal, oblique slickenside lineation (Fig. 13b).

Below the dike, a wide fault damage zone can be traced. It consists of tectonic breccia and fault gouge. Within the breccia, coarser and finer-grained parts are observed (Fig. 13c and d). The coarser-grained breccia is composed of cm-scale, sharp, light-gray dolomite clasts, whereas the fine-grained is made up by mm-scale clasts. The breccia is cemented by light, yellowish-gray sparry calcite. The proportion of the clasts within the cement is low, around 20%–50%. The fault gouge is light- to medium-gray dolomite powder, clay-sized particles of dolomite or clay minerals, and

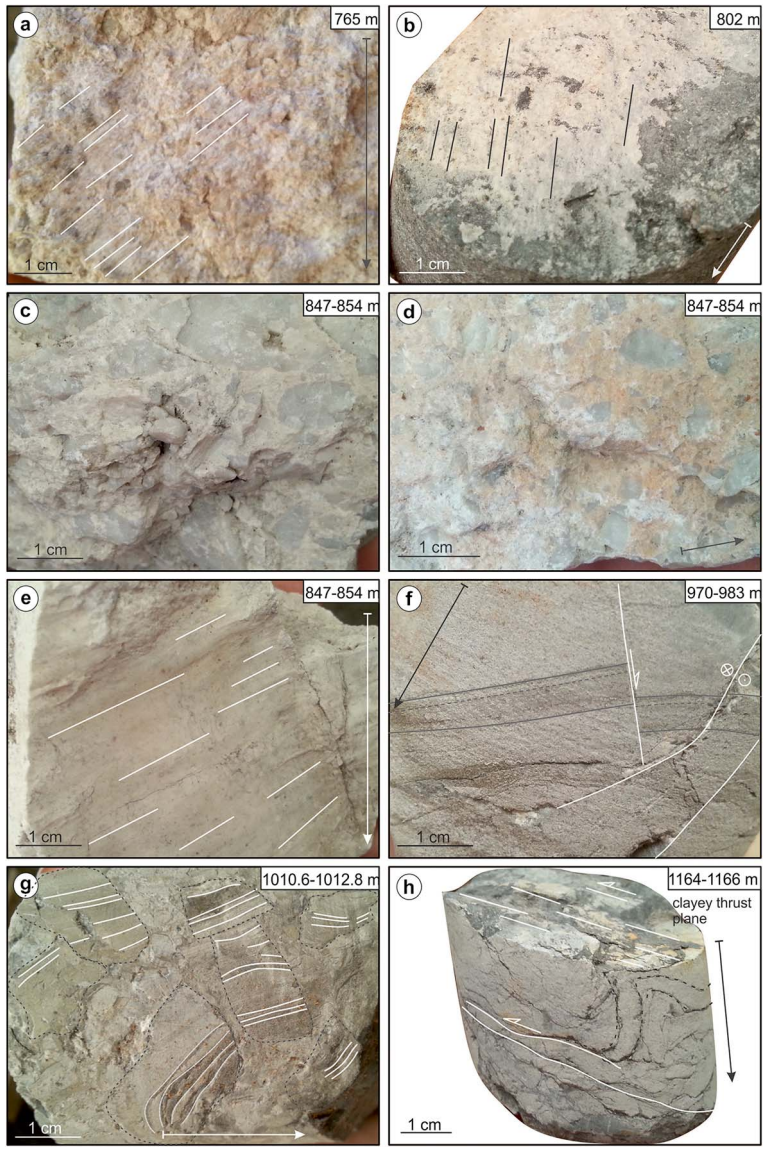

Fig. 13
Structural observations in the Budaörs-1 borehole. Gray arrows show downward direction. (a) Oblique slickenside lineation on a steep cataclastic fault surface. (b) Along-strike lineation on a flatly dipping fault plane. Coarse-grained (c) and fine-grained (d). Matrix-reach cataclasite of the tectonic zone penetrated at 847–854 m. (e) Oblique-slip lineation on a steep fault plane. (f) Subvertical and steeply dipping normal fault and strike-slip fault in the well-bedded, lower dolomite unite. (g) Mosaic-type breccia with steeply dipping clasts. (h) Supposed detachment fold and connected low-angle thrust surfaces with dip-slip lineation

some mm-scale dolomite clasts. It is an incoherent gouge or fine-grained cataclasite. The breccia is crosscut by several steep fault planes with oblique to subhorizontal slickenside lineation (Fig. 13e). In the lower part of the Budaörs Dolomite, several other tectonic breccia zones are detected with similar breccias and steeply dipping fault planes (e.g., ~882, 930–933 m). The only dip-slip movement was measured at 882 m, on a moderately dipping fault plane (~45°).

A breccia zone also occurs at the contact between the Budaörs Formation and the Mátyáshegy Formation. This is characterized by a grain-supported texture with calcite cement. The breccia is made up by light- and medium-gray, angular, mm- to cm-scale dolomite clasts. The lighter clasts may derive from the upper, whereas the darker ones from the lower dolomite unit.

In the 970- to 983-m interval, an oblique-slip fault was detected with sinistral and reverse slip components (Fig. 13f). This set of faults crosscuts an earlier, normal fault generation. The sense of movement along the normal fault is indicated by the displaced darker laminae within the light-gray dolomite. The branches of the younger fault are quite steep with oblique slickensides. The most interesting deformation features within the lower dolomite unit occur at 1,010 and 1,164 m. At 1,010-m depth, a few meter thick tectonic breccia is present. The clasts of the breccia have sedimentary lamination indicating locally steep dip for the mosaic-type breccia clasts (Fig. 13g). Between 1,138 and 1,140 m, a steeply dipping oblique-slip fault was detected. The lowermost observed structural elements are flat-lying clayey surfaces with dip-slip slickenside lineation, and a detachment fold (?) (Fig. 13h). The lower detachment surface for the fold is parallel to the lineated thrust plane. Both surfaces are dark-gray clay-rich horizons within the more competent, light-gray dolomite.

Discussion

The new studies confirmed the stratigraphic assignment of Nagy et al. (1967) for the upper dolomite unit; the Budaörs Dolomite Formation according to the current lithostratigraphic subdivision. The dasycladalean alga flora constrains a late Anisian to Ladinian age for the exposed section of the Budaörs Dolomite of 500–600 m stratigraphic thickness. The succession is probably made up of a cyclic alternation of peritidal and shallow subtidal beds throughout the section. However, due to the intense tectonic fragmentation and recrystallization, the original sedimentary texture is partially or completely destructed in several segments of the succession.

With regard to the andesite dike, the results of the U–Pb age determination deserve particular attention. The measurements provided a Carnian age (~233 Ma), close to the age inferred in the first report on the well by Horváth and Némedi-Varga (1965), which correlated the volcanic dike with the Ladinian volcanic tuffs of the Bakony–Balaton Highland region. The new results, however, are in contrast with the interpretation of Nagy et al. (1967). Based on the occurrence of a remarkable amount of andesite clasts in the basal conglomerate of the Upper Eocene, these authors considered the andesite

Eocene in age. This opinion was followed by Wein (1977) and later Korpás and Kovácsvölgyi (1996). K/Ar age determination of the dike rocks yielded very scattered values between 25 and 186 Ma (Balogh et al. 1983; Kubovics 1985; Kubovics et al. 1990). Due to the strong alteration of the andesite, these age data cannot be considered as relevant; they should be much younger than the original ones. However, the data suggest pre-Eocene volcanism (Gyalog and Horváth 2004). Horváth and Tari (1987) argued for the Middle Triassic age of the andesite clasts within the Eocene basal conglomerate frequently found in the Buda Hills.

The new zircon U–Pb measurements provided the first reliable and decisive age data for the andesite dike intersected in core Bö-1. This dike is a preserved remnant of the Carnian volcanism, which took place after the deposition of the Budaörs Dolomite Formation. Age data for the Pietra Verde-type rhyodacitic tuffs of the Balaton Highland (late Anisian; ~241 Ma; Pálfy et al. 2003) derived from distal volcanic centers (probably from the South Alpine realm) indicate a significantly older volcanic activity. In addition to the late Anisian to Ladinian silicic volcanic deposits ("pietra verde" tuffs), and Ladinian andesitic to basaltic lava flows, late Ladinian and Carnian volcanic activities were also reported from the Dolomites (Bosellini et al. 1996, 2003; Mundil et al. 2010). Mafic dike swarms and diatremes cutting through the late Anisian–Ladinian platform carbonates ("Latemar limestone" of the Schlern Formation) were reported from the Latemar area (Budai et al. 2005; Németh and Budai 2009).

No age-diagnostic fossils were previously found in the finely crystalline dolomite unit encountered in the lower part of the core. Nagy et al. (1967) assumed a late Carnian age of the unit on the basis of lithologic features (medium- to dark-gray color, clay content), but this age assignment was understandably very uncertain. Palynostratigraphic studies of the present project provided evidence for a late Carnian to early Norian age of the upper part of the lower unit showing lithologic affinity with the Mátyáshegy Formation. This result verified the assumption of Nagy et al. (1967) and reinforced their statement on the significance of the tectonic contact between the upper unit (Budaörs Formation) and the lower unit (Mátyáshegy Formation).

From a structural point of view, in the Bö-1 well, an older formation (Anisian–Ladinian) is juxtaposed on a younger one (late Carnian–early Norian), suggesting a thrust contact. However, our observations regarding the dip angle of the fault planes and the plunge of the slickenside lineation do not support the idea of a thrust. The majority of the measured fault planes are steep (i.e., steeper than 60°) surfaces with oblique slickenside lineation, which refer to strike-slip faulting. Juxtaposition of the formations indicate reverse motion, thus transpressional movements along a strike-slip fault zone is the most probable contact type for the intersected structural boundary. The boundary between the cherty dolomite (Mátyáshegy Formation) and the platform dolomite (Budaörs Formation) is an E–W striking surface (Fig. 1). Taking into account the superposition of the formations, an E–W-oriented oblique-slip fault with a northern reverse component can be suggested. To the N–NW from this fault zone, an E–NE dipping southwestern limb of a large-scale syncline was mapped (Wein 1977). Within

this fold limb, the stratigraphic contact between the Budaörs and Mátyáshegy Formations is located to the WNW of the Bö-1 borehole, suggesting sinistral transpression along the postulated E–W striking oblique-slip fault (Fig. 14a).

An even more complex geological situation becomes apparent, if the immediate vicinity of the borehole is taken into account. A few hundred meters to the NW of the borehole, on the southeastern ridge of the Tűzkő Hill (Figs 1 and 3), well-bedded gray dolomite crops out, which is similar to that explored in the lower part of the core in both microfacies and age (late Carnian; Karádi et al. 2016). This dolomite dips gently toward the SSW. If the presumable correlation of these beds with the lower unit of the borehole is correct, a sudden and considerable change in the dip angle is needed (Fig. 14a). This means that the rocks of the Mátyáshegy Formation are dragged into the deformation zone. This may be a possible solution, however, almost vertical bedding should be assumed, confirmed neither by field data nor by our observations on the core material of the well. The detected dip values were usually around 20°–40°, which is not steep enough to connect the lower unit of the core with the surface outcrops of the Mátyáshegy Formation.

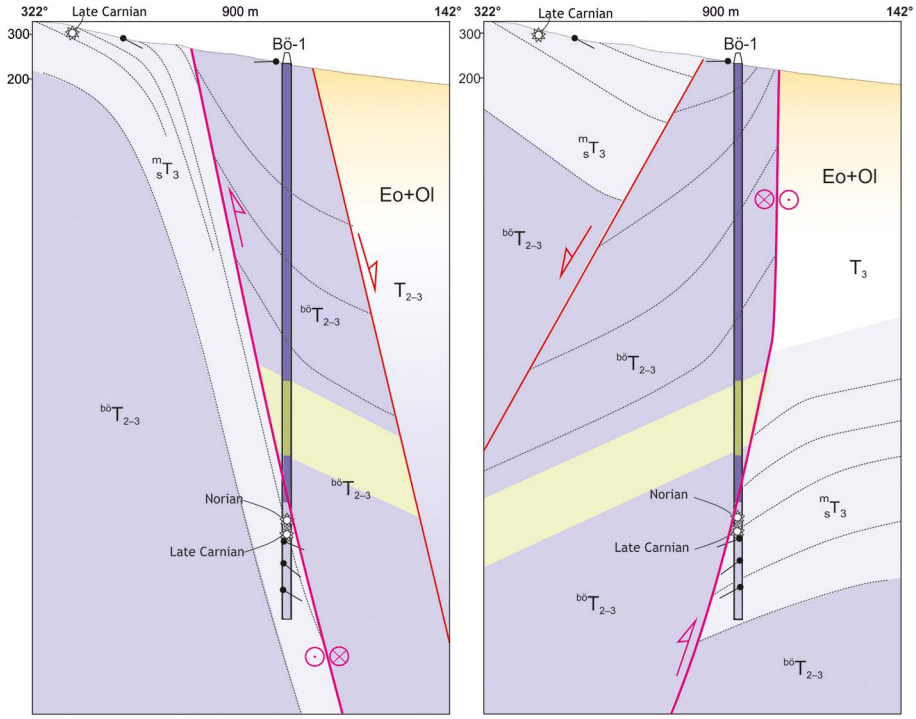

Fig. 14
Suggested alternative structural model sections of the Budaörs-1 borehole and the surrounding area. Cross-section line is indicated in Fig. 3

An alternative model is presented in Fig. 14b. An equally E–W striking oblique-slip fault is suggested for the major thrust contact, which juxtaposes the older Budaörs Dolomite and the younger Mátyáshegy Formation in the borehole. However, both the dip direction and the kinematics of this fault are different from that of model A (Fig. 14a and b). In model B, a right-lateral transpressional fault is suggested with top-to-southeast transport direction. The observed gentle dip values support this model. In this case, the contact of the two units on the Tűzkő Hill (Fig. 3) is also of tectonic origin. In contrast to model A, a NW dipping fault with normal movement is suggested (Fig. 14b). The same type of fault contact was postulated by Wein (1977).

As to the time constraints of the fault movements, the two proposed models can be evaluated as follows. Reverse–sinistral motion could have taken place along the E–W striking steep fault of model A in a stress field characterized by NE–SW compression and perpendicular extension. According to previous structural measurements and stress field analysis (Fodor et al. 1994, 2013; Pocsai and Csontos 2006), the Transdanubian Range was dominated by NE–SW to N–S compression during the Barremian to early Albian time. This means that the postulated reverse–sinistral movement took place right after the formation of the NW–SE directed map-scale syncline (Wein 1977; Fodor et al. 1994).

In contrast, the dextral transpressional motion suggested by model B can be fit into a stress field with NW–SE compression and NE–SW extension. According to the detailed works of Fodor et al. (1994), Magyari (1998), and Fodor and Magyari (2002), ENE–WSW striking dextral transpressional faults of the Budaörs tectonic zone were formed during the Eocene, when the stress regime was characterized by NW–SE directed maximal, and perpendicular minimal horizontal stress axes. Thus, model B would fit much better into the Eocene fault pattern (Fodor et al. 1994). This stress field was characteristic of the northeastern part of the Transdanubian Range from late Eocene till the earliest Miocene, thus the transpressional contact of model B most probably developed during this interval.

From the early Miocene, the syn-rift subsidence of the Pannonian Basin started. The characteristic fault pattern for this event is NW–SE striking normal faults. These structures usually cause a pronounced change in the surface morphology. The relatively narrow ridge of the Tűzkő Hill is bound by such normal faults both on the NE and SW sides (Fig. 3). On the topographic section of Fig. 13, there is no sign of any abrupt change in the slope angle, which provides an additional argument for the older age of the reverse fault contact.

Conclusions

Revisiting of the core material in the Bö-1 well yielded important results on the stratigraphic assignment and sedimentological characteristics of the intersected Triassic carbonates and provided valuable data on the age and petrography of an andesite dike. These data are crucial to better understand the Middle to Late Triassic evolution of the northeastern part of the Transdanubian Range and the tectonic setting of the Buda Hills.

The new studies confirmed the lithostratigraphic assignment of the upper dolomite unit to the Budaörs Dolomite Formation and the dasycladalean alga flora proved its late Anisian to Ladinian age assignment.

The U–Pb age determination performed on zircon crystals revealed a Carnian age (~233 Ma) of the andesite dike intersected within the Budaörs Dolomite and proved the existence of a Carnian volcanic activity in this area after the deposition of the Budaörs Dolomite.

Palynostratigraphic studies provided evidence for a late Carnian to early Norian age of the upper part of the lower unit (Mátyáshegy Formation) and confirmed a tectonic contact between the Mátyáshegy and Budaörs Dolomite Formations.

Based on structural studies, two alternative models are considered for the structural style and kinematics of the contact zone between the Budaörs and Mátyáshegy Formations. Model A suggests a Cretaceous age for the juxtaposition, along E–W striking sinistral transpressional fault. Model B postulates dextral transpression and an Eocene age for the deformation. Although none of these scenarios can be entirely excluded, the latter one is more supported by the scattered dip data observed in the well.

Acknowledgements

This study was supported by the Hungarian National Science Fund (OTKA) under grant number K 113013 (to L. Fodor). The authors express their gratitude to the Hungarian Office for Mining and Geology for permission to study the archived Budaörs-1 core materials and the Geological and Geophysical Institute of Hungary for providing previously prepared thin sections. Suggestions and comments of the reviewers Gábor Tari and Árpád Magyari considerably improved the manuscript.

References

Balogh, K., E. Árva-Sós, Gy. Buda 1983: Chronology of granitoid and metamorphic rocks of Transdanubia (Hungary). – Anuarul Institutului de Geologie şi Geofizică, 61, pp. 359–364.

Bosellini, A., C. Neri, M. Stefani 1996: Geologia delle Dolomiti. Introduzione Geologica. Guida alla Escursione Generale [Geology of the Dolomites. An Introduction. Guide to General Excursion]. – Societa Geologica Italiana, Rome, 120 p.

Bosellini, A., P. Gianolla, M. Stefani 2003: Geology of the Dolomites. – Episodes, 26, pp. 181–185.

Brönniman, P., J.-P. Cadet, L. Zaninetti 1973: Sur la présence d'Involutina sinuosa pragsoides (Oberhauser) (Foraminifère) dans l'Anisien supérior probable de Bosnie-Herzégovine méridionale (Yougoslavie) [On the occurrence of Involutiona sinuosa pragsoides (Oberhauser) (Foraminifera) in the upper Anisian of southern Bosnia-Herzegovina (Yugoslavia)]. – Rivista Italiana di Paleontologia e Stratigrafia, 79/3, pp. 301–336.

Budai, T., K. Németh, O. Piros 2005: Középső-triász platformkarbonátok és vulkanitok vizsgálata a Latemar környékén; Dolomitok, Olaszország [Middle Triassic platform carbonates and volcanites in the Latemar area; Dolomites, Italy]. – Annual Report of the Geological Institute of Hungary, 2004, pp. 175–188. (in Hungarian)

Chablais, J., R. Martini, F. Kobayashi, G.M. Stampfli, T. Onoue 2011: Upper Triassic foraminifers from Panthalassan carbonate buildups of Southwestern Japan and their paleobiogeographic implications. – Micropaleontology, 57/2, pp. 93–124.

Csontos, L., A. Nagymarosy 1998: The Mid-Hungarian line: A zone of repeated tectonic inversions. – Tectonophysics, 297, pp. 51–71.

Csontos, L., A. Vörös 2004: Mesozoic plate tectonic reconstruction of the Carpathian region. – Palaeogeography, Palaeoclimatology, Palaeoecology, 210, pp. 1–56.

Dunkl, I., T. Mikes, K. Simon, H. von Eynatten 2008: Brief introduction to the Windows program Pepita: Data visualization, and reduction, outlier rejection, calculation of trace element ratios and concentrations from LA-ICP-MS data. – In: Sylvester, P. (Ed): Laser Ablation ICP-MS in the Earth Sciences: Current Practices and Outstanding Issues, Short Course. Mineralogical Association of Canada, Québec, Vol. 40, pp. 334–340.

Farics, É., S. Józsa, J. Haas 2015: A Budai-hegység felső-eocén összletének bázisán települő lávakőzet- és tufaklasztokat tartalmazó törmelékes üledékes kőzetek petrográfiai jellegei [Petrographic features of lava rock and tuff clast-bearing sedimentary rocks at the base of the Upper Eocene succession in the Buda Hills]. – Földtani Közlöny, 145/4, pp. 331–350. (in Hungarian)

Fodor, L., Á. Magyari 2002: Késő-eocén-miocén szerkezetalakulás és üledékképződés a Sas-hegyen [Late Eocene–Miocene structural evolution and sedimentation on the Sas Hill, Budapest, Hungary]. – Földtani Közlöny, 132/2, pp. 247–264. (in Hungarian)

Fodor, L., Á. Magyari, A. Fogarasi, K. Palotás 1994: Tercier szerkezetfejlődés és késő paleogén üledékképződés a Budai-hegységben. A Budai vonal új értelmezése [Tertiary tectonics and Late Paleogene sedimentation in the Buda Hills, Hungary. A new interpretation of the Buda Line]. – Földtani Közlöny, 124/2, pp. 129–305. (in Hungarian)

Fodor, L., O. Sztanó, Sz. Kövér 2013: Pre-conference field trip: Mesozoic deformation of the northern Transdanubian Range (Gerecse and Vértes Hills). – Acta Mineralogica-Petrographica, Field Guide Series, 31, pp. 1–34.

Frei, D., A. Gerdes 2009: Precise and accurate in situ U–Pb dating of zircon with high sample throughput by automated LA-SF-ICP-MS. – Chemical Geology, 261, pp. 261–270.

Gale, L. 2012: Rhaetian foraminiferal assemblage from the Dachstein Limestone of Mt. Begunjščica (Košuta Unit, eastern Southern Alps). – Geologija, 55/1, pp. 17–44.

Gyalog, L., I. Horváth (Eds) 2004: Geology of the Velence Hills and the Balatonfő. – Regional Map Series of Hungary, Geological Institute of Hungary, Budapest, 316 p.

Haas, J., S. Kovács, L. Krystyn, R. Lein 1995: Significance of Late Permian–Triassic facies zones in terrane reconstructions in the Alpine–North Pannonian domain. – Tectonophysics, 242, pp. 19–40.

Haas, J., L. Korpás, Á. Török, L. Dosztály, F. Góczán, M. Hámor-Vidó, A. Oravecz-Scheffer, E. Tardi-Filácz 2000: Felső-triász medece- és lejtőfáciesek a Budai-hegységben – A Vérhalom téri fúrás vizsgálatának tükrében [Upper Triassic basin and slope facies in the Buda Mts. – Based on study of core drilling Vérhalom tér, Budapest]. – Földtani Közlöny, 130/3, pp. 371–421. (in Hungarian)

Hips, K., J. Haas, Zs. Poros, S. Kele, T. Budai 2015: Dolomitization of Triassic microbial mat deposits (Hungary): Origin of microcrystalline dolomite. – Sedimentary Geology, 318, pp. 113–129.

Hofmann, K. 1871: A Buda-Kovácsi hegység földtani viszonyai (Die geologischen Verhältnisse des Ofen-Kovácsier Gebirges) [The geological situation of the Buda-Kovacs Mountains]. – Annals of the Hungarian Royal Geological Institute, 1/2, pp. 199–273. (in Hungarian)

Horusitzky, F. 1959: Die triassischen Bildungen des Budaer Gebirges. – In: Balogh, K. (Ed): Führer zu den Ausflügen, Konferenz über das Ungarische Mesozoikum [Field Guide, Conference on the Hungarian Mesozoic]. Geological Institute of Hungary, Budapest, pp. 3–13.

Horváth, E., G. Tari 1987: Middle Triassic volcanism in the Buda Mountains. – Annales Universitatis Scientiarum Budapestiensis, Sectio Geologica, 27, pp. 3–16.

Horváth, G., Z. Némedi-Varga 1965: Budaörs-1 sz. kutatófúrás földtani ismertetése [Geological structure of the Budaörs-1 borehole]. – Manuscript, Hungarian State Geological, Geophysical and Mining Databank, 1346/11. (in Hungarian)

Jackson, S., N. Pearson, W. Griffin, E. Belousova 2004: The application of laser ablation-inductively coupled plasma-mass spectrometry to in situ U–Pb zircon geochronology. – Chemical Geology, 211, pp. 47–69.

Karádi, V., P. Pelikán, J. Haas 2016: A Budai-hegység triász medence fáciesű dolomitjainak conodonta vizsgálatokon alapuló korbesorolása [Conodont biostratigraphy of Upper Triassic dolomite of the Buda Hills; Transdanubian Range, Hungary]. – Földtani Közlöny, 146/4, pp. 371–386. (in Hungarian)

Koehn-Zaninetti, L. 1969: Les Foraminifères du Trias de la région de l'Almtal (Haute-Autriche) [Foraminifers of the Triassic of the Almtal (Upper Austria)]. – Jahrbuch der Geologischen Bundesanstalt, Sonderband, 14, pp. 1–155.

Kolar-Jurkovšek, T., A. Ga dzicki, B. Jurkovšek 2005: Conodonts and foraminifera from the "Raibl Beds" (Carnian) of the Karavanke Mountains, Slovenia: Stratigraphical and palaeobiological implications. – Geological Quarterly, 49/4, pp. 429–438.

Korpás, L., S. Kovácsvölgyi 1996: Eltemetett paleovulkán a Budai-hegység DK-i előterében [Buried Paleogene volcano in the SE foreland of the Buda Hills]. – Földtani Közlöny, 126/2–3, pp. 155–175. (in Hungarian)

Kubovics, I. 1985: Mesozoic magmatism of the Transdanubian Mid-Mountains. – Acta Geologica Hungarica, 28/3–4, pp. 141–164.

Kubovics, I., Cs. Szabó, Sz. Harangi, S. Józsa 1990: Petrology and petrochemistry of Mesozoic magmatic suites in Hungary and adjacent areas – An overview. – Acta Geodaetica, Geophysica et Montanistica Hungarica, 25/3–4, pp. 345–341.

Kutassy, E. 1927: Beiträge zur Stratigraphie und Paläontologie der alpinen Triasschichten in der Umgebung von Budapest [Contributions on the stratigraphy and palaeontology of the alpine Triassic in the Budapest region]. – Annals of the Hungarian Royal Geological Institute, 27, pp. 107–175.

Ludwig, K.R. 2012: User's manual for Isoplot 3.75: A geochronological Toolkit for Microsoft Excel. – Berkeley Geochronology Center, Special Publication, 4, 70 p.

Magyari, Á. 1994: Késő-eocén transzpresszió a Budaörsi-hegyekben [Late Eocene transpression in the Budaörs Hills]. – Földtani Közlöny, 124/2, pp. 155–173. (in Hungarian)

Magyari, Á. 1996: Eocén szinszediment tektonikai jelenségek és üledékképződésre gyakorolt hatásaik a Budai-hegységben [Eocene synsedimentary tectonics of the Buda Hills and their influence on sedimentation]. – PhD dissertation, Eötvös University, Budapest, 289 p. (in Hungarian)

Magyari, Á. 1998: Törökugrató: késő-eocén szinszediment pozitív virágszerkezet a Budai-hegység DNY-i peremén [Törökugrató Hill: Late Eocene positive flower structure on the southwestern part of the Buda Mountains, Budapest]. – Földtani Közlöny, 128/4, pp. 555–572. (in Hungarian)

Mundil, R., J. Pálfy, P.R. Renne, P. Brack 2010: The Triassic timescale: New constraints and a review of geochronological data. – In: Lucas, S.G. (Ed): The Triassic Timescale, Geological Society, Special Publications, London, Vol. 334, pp. 41–60.

Nagy, E., G. Nagy, F. Széky 1967: A Budaörs-1-sz. alapfúrás [Exploratory drilling Budaörs Nr. 1]. – Annual Report of the Geological Institute of Hungary, 1965, pp. 289–297. (in Hungarian)

Németh, K., T. Budai 2009: Diatremes cut through the Triassic carbonate platforms in the Dolomites? Evidences from and around the Latemar, Northern Italy. – Episodes, 32/2, pp. 74–83.

Oberhauser, R. 1960: Foraminiferen und Mikrofossilien "incertae sedis" der ladinischen und karnischen Stufe der Trias aus den Ostalpen und aus Persien [Foraminifers and microfossils "incertae sedis" of the Ladinian and Carnian (Triassic) of the Eastern Alps and Persia]. – Jahrbuch der Geologischen Bundesanstalt, Sonderband, 5, pp. 5–46.

Oravecz-Scheffer, A. 1987: A Dunántúli-Középhegység triász képződményeinek foraminiferái [Triassic Foraminifers of the Transdanubian Central Range]. – Geologica Hungarica Series Paleontologica, 50, pp. 1–331. (in Hungarian)

Paces, J.B., J.D. Miller 1993: Precise U–Pb ages of Duluth Complex and related mafic intrusions, northeastern Minnesota: Geochronological insights into physical, petrogenetic, paleomagnetic and tectonomagmatic processes associated with the 1.1 Ga midcontinent rift system. – Journal of Geophysical Research, 98, pp. 13997–14013.

Pálfy, J., R.R. Parrish, K. David, A. Vörös 2003: Mid-Triassic integrated U–Pb geochronology and ammonoid biochronology from the Balaton Highland (Hungary). – Journal of the Geological Society, 160, pp. 271–284.

Pelech, O., J. Soták, J. Hók 2012: Geological setting of the Patrovec block in the Považský Inovec Mts., Western Carpathians. – Mineralia Slovaca, 44, pp. 231–240.

Piller, W. 1978: Involutinacea (Foraminifera) der Trias und der Lias [Involutinacea (Foraminifera) of the Triassic and Liassic]. – Beiträge zur Paläontologie von Österreich, 5, pp. 1–164.

Piros, O., N. Preto 2008: Dasycladalean algae distribution in ammonoid-bearing Middle Triassic platforms (Dolomites, Italy). – Facies, 54, pp. 581–595.

Pocsai, T., L. Csontos 2006: Late Aptian–Early Albian syn-tectonic facies-pattern of the Tata Limestone Formation (Transdanubian %Range, Hungary). – Geologica Carpathica, 57/1, pp. 15–27.

Rettori, R. 1994: Replacement name Hoyenella, gen. n. (Triassic Foraminiferida, Miliolina) for Glomospira sinensis Ho, 1959. – Bollettino della Società Paleontologica Italiana, 33/3, pp. 341–343.

Rettori, R. 1995: Foraminiferi del Trias inferior e medio della Tetide: revisione tassonomica, stratigrafia, ed interpretazione filogenética [Foraminifers of the Lower and Middle Triassic of the Tethys: Taxonomic revision, stratigraphy and phylogenetic interpretation]. – Publications du Département de Géologie et Paléontologie, Université de Genève, 18, 147 p.

Rychliński, T., D.K. Ivanova, P. Jaglarz, I.I. Bucur 2013: Benthic foraminifera and calcareous algae from the Anisian–Norian succession in the Tatras (Poland and Slovakia): New data from High Tatric and Križna units. – Studia UBB Geologia, 58/1, pp. 21–43.

Schafarzik, F., A. Vendl 1929: Geológiai kirándulások Budapest környékén [Geological excursions in the environs of Budapest]. – Hungarian Royal Geological Institute, Budapest, 341 p. (in Hungarian)

Schmidt, Th., J. Blau, M. Kázmér 1991: Large-scale strike-slip displacement of the Drauzug and the Transdanubian Mountain in early Alpine history: Evidence from Permo-Mesozoic facies belts. – Tectonophysics, 200, pp. 213–232.

Schréter, Z. 1912: Harmadkori és pleisztocén hévforrások tevékenységének nyomai a Budai hegyekben [Traces of activities of Tertiary and Pleistocene thermal springs in the Buda Hills]. – Annals of the Hungarian Royal Geological Institute, 19/5, pp. 179–231. (in Hungarian)

Schréter, Z., E. Szőts, F. Horusitzky, B. Mauritz 1958: Budapest és környékének geológiája [Geology of Budapest and its surroundings].– In: Pécsi, M. (Ed): Budapest természeti képe. Akadémiai Kiadó, Budapest, pp. 35–145. (in Hungarian)

Sláma, J., J. Košler, D.J. Condon, J.L. Crowley, A. Gerdes, J.M. Hanchar, M.S.A. Horstwood, G.A. Morris, L. Nasdala, N. Norberg, U. Schaltegger, B. Schoene, M.N. Tubrett, M.J. Whitehouse 2008: Plešovice zircon – A new natural reference material for U–Pb and Hf isotopic microanalysis. – Chemical Geology, 249, pp. 1–35.

Sloman, L.E. 1989: Triassic shoshonites from the Dolomites, northern Italy: Alkaline arc rocks in a strike-slip setting. – Journal of Geophysical Research, 94, pp. 4655–4666.

Streckeisen, A.L. 1978: IUGS subcommission on the systematics of igneous rocks. Classification and nomenclature of volcanic rocks, lamprophyres, carbonatites and melilite rocks. Recommendations and suggestions. – Neues Jahrbuch für Mineralogie, 141, pp. 1–14.

Végh-Neubrandt, E. 1974: Stratigraphische Lage der Triaskomplexe des Budaer Gebirges [Stratigraphy of the Triassic of the Buda Hills]. – Annales Universitatis Scientiarum Budapestiensis, Sectio Geologica, 17, pp. 287–301.

Végh-Neubrandt, E. 1982: Triassische Megalodontaceae. Entwicklung, Stratigraphie und Paläontologie [Triassic Megalodontaceae. Evolution, Stratigraphy and Palaeontology]. – Akadémiai Kiadó, Budapest, 526 p.

Vendl, A. 1923: Reambuláció Budaörs környékén [Investigations in the surroundings of Budaörs]. – Annual Report of the Hungarian Royal Geological Institute, 1917–1919, pp. 42–47. (in Hungarian)

Wein, Gy. 1977: A Budai-hegység tektonikája [Tectonics of the Buda Mts.]. – Geological Institute of Hungary, Budapest, 76 p. (in Hungarian)

Wiedenbeck, M., P. Allé, F. Corfu, W.L. Griffin, M. Meier, F. Oberli, A. von Quadt, J.C. Roddick, W. Spiegel 1995: Three natural zircon standards for U–Th–Pb, Lu–Hf, trace element and REE analyses. – Geostandards Newsletter, 19, pp. 1–23.